Proceedings of the 1999 IEEE/ASME
International Conference on Advanced Intelligent Mechatronics
September 19-23, 1999 • Atlanta, USA

Design Analysis of a Grating Interferometer Sensor for HDD Servo-Track Writing

Harry Garner†, Kok-Meng Lee†, Lin Guo‡

Abstract–**A grating interferometer (GI) system for the measurement of a hard disk drive (HDD) actuator arm during the servo-track writing (STW) process has been designed and analyzed. Attractive features of this GI based system over current measurement systems such as the mechanical and optical push-pin techniques are that it does not require contact with the actuator arm and only needs a single servo loop to control the actuator arm position. In this paper, the theory necessary for the design of a GI based system to perform a non-contact direct measurement of a HDD actuator arm for use in STW will be presented. First, the theoretical background related to the linear type GI is presented, and this theory is extended to the measurement of the angular displacement of a HDD actuator arm using a linear grating. Finally, experimental results with a prototype GI measurement system are presented and discussed.**

Index terms-- **grating interferometer, high-resolution measurement, servo-track writing, metrology, CCD camera**

I. Introduction

In recent years, measurement systems based on the grating interferometer (GI) principle have been used in a number of measurement applications. The measurement capability of such systems gives them much promise as replacements for conventional slit type encoders. Their high resolution, stability under changing environmental conditions, and compact design also gives them certain advantages over conventional interferometers [1][2]. GI systems are typically used to measure linear or angular displacements using an appropriate type of grating structure. With a thorough understanding of the theory related to the operating principle of the GI, it is possible to measure other types of displacements using a linear grating.

An application in which high-resolution measurement plays a significant role is hard disk drive (HDD) servo-track writing (STW). To measure the displacement of the read/write head of a HDD, servo information is written onto the surface of the magnetic disk in special servo tracks that act as an embedded encoder system, which makes the high data densities and fast access times of current HDDs possible [4].

†George W. Woodruff School of Mechanical Engineering, Georgia Institute of Technology, Atlanta, GA 30332-0405
Tel: (404)894-7402; email: kokmeng.lee@me.gatech.edu
‡ Maxtor Corporation, 510 Cottonwood Dr, Milpitas, CA 95035

During the STW process the HDD actuator arm must be positioned very accurately to write the servo tracks at the correct locations to achieve the highest track densities possible. To control the arm position a high-resolution measurement system is necessary. Current STW systems rely on conventional interferometers or other optical techniques to measure the actuator arm position. Two commonly used techniques are the mechanical and optical push-pin techniques. The mechanical push-pin approach utilizes an interferometer measurement system and a push-pin in contact with the actuator arm to control the position of the arm. Such an approach has certain disadvantages due to contact between the arm and push-pin. The optical push-pin approach uses an optical measurement technique to eliminate contact with the arm, and uses the HDD voice coil motor to position the arm by tracking the motion of an external optical sensor system. Such a non-contact approach is thought to be optimal for speed and accuracy in the STW process, but it requires two feedback control loops to operate both the HDD voice coil motor and an external actuator to position the optical sensor system [3][6].

To reduce the complexity of the STW measurement system, a GI based system has been proposed to perform a direct non-contact measurement of the HDD actuator arm. In this paper it will be shown that a linear grating can be used to measure the angular displacement of the object to which it is attached using the GI principle. First, a linear GI system will be analyzed, and results of this analysis will be applied to the measurement of the angular displacement of a HDD actuator arm. Finally, experimental results that show the measurement capability of the GI design will be presented and discussed.

II. Grating Interferometer Background

A GI is a type of interferometer that consists of a collimated coherent light source, diffraction grating configuration, and a suitable detector for measuring the phase shift of the interference fringe pattern. It can be used to make high-resolution relative displacement measurements by relating the phase shift of a fringe pattern to the relative displacement between the light source and the diffraction grating configuration.

0-7803-5038-3/99/$10.00 © 1999 IEEE

A. *Fringe Pattern Determination for Single Grating*

To determine the relative displacement between the diffraction grating and light source, the phase shift of the interference fringe pattern must be related to this relative displacement. Figure 1 shows a single grating configuration with a collimated light beam incident from above.

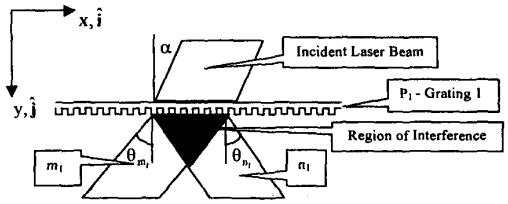

Figure 1. Grating Interferometer With Single Grating

As shown in Figure 1, where any two diffracted beams from the grating overlap an interference fringe pattern is formed within some region of interference (ROI) with properties determined by the incident beam and the grating. The intensity of this fringe pattern can be determined using fundamental principles of optics by modeling each diffracted beam from the grating as a plane wave travelling in the direction of the diffracted beam including effects from the periodic grating structure [7]. The displacement of the grating causes a phase shift of the diffracted beams, which is given by

$$\phi_m = \frac{2\pi m x_1}{P_1} \qquad (1)$$

Equation (1) relates the phase shift of the m diffracted order, the location of Grating 1, x_1, and the grating period P_1 [8]. This means that as Grating 1 moves through one of its periods the phase of the m diffracted beam will be shifted by $2\pi m$ due to the Doppler shift produced by the moving grating [9]. This relationship is very important because it allows the phase shift of the diffracted beams to be related to the relative motion between the coherent light source and the diffraction gratings making displacement measurement with a GI system possible.

As indicated in Figure 1, there is a ROI where the m_1 and n_1 diffracted beams overlap. In general, the intensity of the fringe pattern formed in this ROI can be found by taking the modulus squared of the sum of the complex amplitudes of the plane waves present in this ROI. It is straightforward to show that the intensity of this interference fringe pattern is given by

$$I_{m_1 n_1}(x,y) = 2\left(A_{m_1}\right)^2\left\{1+\cos\left[\frac{2\pi}{P_{D1}}x+\frac{2\pi}{P_{S1}}x_1+\frac{2\pi}{P_{Dy}}y\right]\right\} \qquad (2)$$

with beam amplitudes A_{m_1} assumed real and equivalent and the following periods corresponding to periods of interference fringes in x (P_{D1}) and y (P_{D1y}) directions and period of the fringe phase shift due to grating motion (P_{S1}) have been defined as

$$P_{D1} = \frac{P_1}{n_1 - m_1} \quad (3) \qquad P_{D1y} = \frac{\lambda}{\cos\theta_{n_1} - \cos\theta_{m_1}} \quad (4) \qquad P_{S1} = \frac{P_1}{n_1 - m_1} \quad (5)$$

Equation (2) gives the relationship between the intensity of the fringes and the location of the grating in the x direction. If the grating moves, x_1 will change causing a phase shift of the fringe pattern proportional to the grating displacement. The relation between the fringe pattern phase shift and the grating displacement can be determined by defining the phase of the fringe pattern as the term that depends on the grating displacement, which is

$$\Phi_1 = \frac{2\pi}{P_{S1}}x_1 \qquad (6)$$

Equation (6) shows that as Grating 1 moves through a distance P_{S1} the fringe pattern will shift through one of its periods. The Grating 1 displacement corresponding to a particular phase can be found by inverting Eq. (6). In practice, it is useful to consider an incremental displacement due to an incremental phase difference given by

$$\Delta x_1 = \frac{P_{S1}}{2\pi}\Delta\Phi_1 \qquad (7)$$

Using Eq. (7) the incremental displacement of Grating 1 can be recovered from an incremental phase shift of the fringe pattern. Equation (2) also shows that as the distance from the gratings increases there will be a phase shift due to the variation of y with an appropriate period. It is interesting to note that P_{D1y} will be infinite when the angle of incidence to Grating 1 is zero. This means that there will be no phase shift as y is varied, which makes such a GI insensitive to out-of-plane displacements.

The resolution of a single grating GI is determined primarily by Eq. (5). For positive and negative first order diffracted beams Eq. (5) will be half the grating period. Therefore, the resolution can only be increased by reducing the grating period. In practice, it is not possible to make the grating period arbitrarily small because the size of the detector element used to sample the fringe pattern must be one fourth the period of the fringe pattern. It will be shown in the following sections that a GI system with two gratings can be used to form an interference pattern with a period suitable for some detector element size.

B. *Dual Grating Configuration*

Figure 2 gives a diagram depicting a typical GI with two gratings. This configuration is analogous to that in

Figure 1, but the ROI is now beyond the second grating. It will be shown that the periods of the two gratings can be chosen such that the period of the interference fringes in the ROI will match a specification based on the detector element size. These grating periods will also be shown to be less than that for a single grating case with the same fringe period, which gives an increase in the resolution.

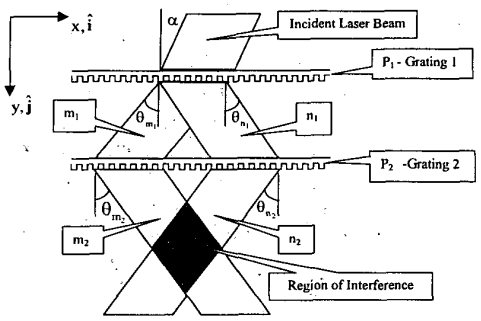

Figure 2. Grating Interferometer with Dual Gratings

The determination of the intensity of the fringe pattern formed by the dual grating configuration is analogous to the single grating case, but with four diffracted beams determining the characteristics of the interference fringe pattern. Using expressions for the complex amplitudes of the m_2 and n_2 diffracted beams from Grating 2 including phase shift terms due to Grating 2, the fringe pattern intensity is given by an expression similar to Eq. (2), which can be shown to be

$$I_{m_2 n_2}(x,y) = 2(A_{m_2})^2\left\{1+\cos\left[\frac{2\pi}{P_{D2}}x+\frac{2\pi}{P_{S1}}x_1+\frac{2\pi}{P_{S2}}x_2+\frac{2\pi y}{P_{D2y}}\right]\right\} \quad (8)$$

where periods corresponding to periods of the interference fringes in the x (P_{D2}) and y (P_{D2y}) directions and the period of the phase shift of the fringes due to the motion of the gratings (P_{S1} and P_{S2}) have been defined as

$$P_{D2} = \frac{P_1 P_2}{P_1(n_2-m_2)+P_2(n_1-m_1)} \quad (9)$$

$$P_{D2y} = \frac{\lambda}{\cos\theta_{n_2}-\cos\theta_{m_2}} \quad (10) \qquad P_{S1} = \frac{P_1}{n_1-m_1}; P_{S2} = \frac{P_2}{n_2-m_2} \quad (11)$$

Equation (8) is analogous to Eq. (2), but is in terms of x_1 and x_2 the locations of both gratings. If either grating moves, x_1 or x_2 will change and cause a phase shift of the fringe pattern proportional to the grating displacements. For a typical GI configuration, one grating is fixed with the other allowed to move. With Grating 1 fixed, the phase shift due to motion of Grating 2 is given by

$$\Phi_2 = \frac{2\pi}{P_{S2}}x_2 \quad (12)$$

Equation (12) can be inverted to find the incremental displacement of Grating 2 that corresponds to a particular incremental phase shift analogous to Eq. (7) given by

$$\Delta x_2 = \frac{P_{S2}}{2\pi}\Delta\Phi_2 \quad (13)$$

C. *Detector Width Compensation*

In practice, the detector used to measure the interference fringe pattern has individual elements of a fixed size, and the periods of the diffraction gratings must be chosen to match the detector element size. To recover the phase from the fringe pattern conveniently, it can be shown that the detector element width δ must be one fourth the period of the interference fringes. For a single grating case Eq. (3) will depend on δ to give

$$P_{D1} = \frac{P_1}{(n_1-m_1)} = 4\delta \quad (14)$$

For the case with positive and negative first order beams interfering, $m_1 = +1$ and $n_1 = -1$ which gives P_1 as

$$P_1 = 8\delta \quad (15)$$

Substituting Eq. (15) in Eq. (5) gives

$$P_{S1} = 4\delta \quad (16)$$

This shows the relationship between the detector element size and the period of the phase shift of the fringe pattern. The size of this period is an indication of the resolution that can be obtained with the single grating configuration, and its dependence on δ shows that the resolution can only be increased if δ is reduced. In practice, the detector element size δ is a fundamental limitation that constrains the resolution of a single grating system.

A similar analysis can be done for a dual grating configuration. The use of the two gratings acts as a way of compensating for the fact that the detector element width is a fundamental design limitation. With the dual grating configuration, the two gratings must be chosen so that the period of the interference fringes meets a certain criteria. Similar to Eq. (14) the period of interference of the fringe pattern is found from Eq. (9) as

$$P_{D2} = \frac{P_1 P_2}{P_1(n_2-m_2)+P_2(n_1-m_1)} = 4\delta \quad (17)$$

As with the single grating case, $m_1 = +1$ and $n_1 = -1$, and $m_2 = -1$ and $n_2 = +1$. This gives Eq. (17) as

$$\frac{P_1 P_2}{2(P_1 - P_2)} = 4\delta \tag{18}$$

For the m_2 and n_2 diffracted beams to overlap, the θ_{m_2} diffracted angle must be positive and the θ_{n_2} diffracted angle must be negative, which requires that the period of Grating 2 be less than that of Grating 1 as given by

$$P_2 < P_1 \tag{19}$$

Equations (18) and (19) are the criteria that must be met by the two grating periods to achieve the detector width compensation (DWC). Unlike Eq. (15) for the single grating case, Eq. (18) is in terms of two grating period values. In practice, the width of the detector elements δ will be a known quantity, and the grating periods satisfying Eq. (18) must be determined. This can be accomplished by iterating over a range of period values and recording period combinations that meet the criteria in Eq. (18). The δ value for the present detector is 10 microns. Table 1 shows grating period combinations that meet the DWC criteria in Eq. (18). Analogous to Eq. (16), the period of the phase shift of the fringe pattern in terms of multiples of the detector element width is also given in Table 1. Compared to the multiple of 4 in Eq. (16) the values for the DWC configuration are significantly less with the first being less by a factor of 5. Therefore, the DWC configuration allows for an increase in the resolution of the GI system because a grating with a smaller period is undergoing displacement.

Table 1. DWC Period combinations with δ multiple

Grating 1 Period (microns)	Grating 2 Period (microns)	Multiple of δ for P_{S2}
20.00	16.00	0.80
45.00	28.80	1.44
48.00	30.00	1.50
80.00	40.00	2.00

D. Fringe Pattern Analysis

With the intensity distribution of the fringe pattern determined as in Eqs. (2) and (8), it is then possible to relate the phase of the fringe pattern with the displacement of the diffraction gratings as in Eqs. (6) and (12). To recover the phase of the fringe pattern from the intensity distribution it is first necessary to sample the intensity distribution using some type of photosensitive detector. The size of the detector elements plays a role in determining the modulation that occurs on each element as the fringe pattern undergoes phase shifts. A commonly used method for extracting the phase from such a fringe pattern utilizes detector elements with a width one fourth the period of the fringe pattern. This gives four unique signal values phase shifted by ninety degrees with respect to each other, which are known as quadrants. The phase of the fringe pattern can be conveniently recovered using the quadrant values and the inverse tangent function [10]. With the recovered phase, Eqs. (6) and (12) can be used to relate the phase to the grating displacement, and Eqs. (7) and (13) to obtain the incremental displacement.

III. Grating Interferometer Applied to HDD

To use a GI system to measure the angular displacement of a HDD actuator arm, a reflection type diffraction grating must be added to the arm assembly to induce a phase shift in the diffracted beams formed from the coherent light source that strikes it. The phase shift will then be related to the displacement of the actuator arm so that a measurement can be performed. This relationship can be derived much like the linear case, but certain geometrical relationships must be considered.

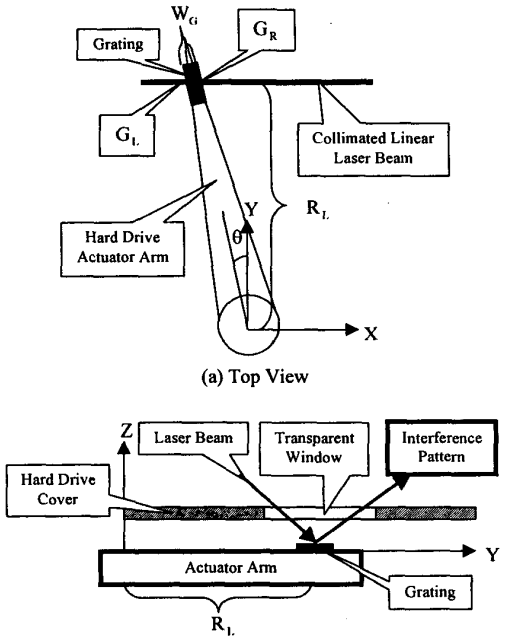

Figure 3. Actuator Arm Geometry

Figure 3 shows the geometry of the arm-mounted grating configuration. In Figure 3(a) a top view of the actuator arm shows the location of the reflection grating with width W_G. As the arm rotates the effective width of the grating illuminated by the light source will vary as a function of the angle of rotation of the actuator arm θ as

$$W_E = \frac{W_G}{\cos\theta} \tag{20}$$

The light source for the GI design is a collimated linear

laser beam that lies along a line given by $Y=R_L$. It extends over the entire range of motion of the actuator arm to maintain illumination of the grating. As shown in Figure 3(b), this laser beam is incident to the HDD from above at some angle and passes through a transparent window in the HDD cover and diffracted beams are reflected from the grating to form the fringe pattern. It is necessary to relate the displacement of the grating along the line illuminated by the light source. The left and right extents of the grating are given by

$$G_L = R_L \tan\theta - \frac{W_G}{2\cos\theta}; \quad G_R = R_L \tan\theta + \frac{W_G}{2\cos\theta} \tag{21}$$

With the necessary geometrical relationships for the arm-mounted grating configuration, it is possible to relate the fringe pattern phase shift and actuator arm displacement. A significant issue related to the grating target is the fact that as the arm rotates the effective period of the grating will vary as a function of the arm orientation given by the following expression

$$P_E = \frac{P_I}{\cos\theta} \tag{22}$$

The phase shift for an arbitrary diffracted beam can be found by recalling the phase shift term for the linear case from Eq. (1) but with an effective period P_E

$$\phi_{m_I}(x_I) = \frac{2\pi}{P_E} m_I x_I \tag{23}$$

Substituting for the effective period from Eq. (22) and the expression relating the displacement of the grating along the linear light source G_L from Eq. (21) for x_I gives

$$\phi_{m_I}(\theta) = \frac{2\pi}{P_I} m_I \left(R_L \tan\theta - \frac{W_G}{2\cos\theta} \right) \cos\theta = \frac{2\pi}{P_I} m_I \left(R_L \sin\theta - \frac{W_G}{2} \right) \tag{24}$$

This is the orientation dependent phase shift of the m_I diffracted beam. For positive and negative first orders with $m_I = +1$ and $n_I = -1$, the net orientation dependent phase shift can be found from the difference between the phase shift of the m_I and n_I diffracted beams as

$$\Psi(\theta) = \phi_{m_I}(\theta) - \phi_{n_I}(\theta) = 2\frac{2\pi}{P_I} R_L \sin\theta \tag{25}$$

Where the constant phase shift given by the W_G terms has been dropped. Using Eq. (25) the angular displacment can be recovered from the phase of the fringe pattern much like the linear displacement case.

IV. Experimental Results

Several experiments have been done to verify the feasibility of the proposed GI design for measuring the angular displacement of a HDD actuator arm. A high-resolution rotary stage with a resolution of 192.3 nanoradians has been used to simulate motion of the actuator arm, and the GI design has also been tested with an actual HDD. With these setups stationary and motion tests have been done to demonstrate system stability and motion tracking capability. The results of the experiments with the rotary stage will now be presented and discussed.

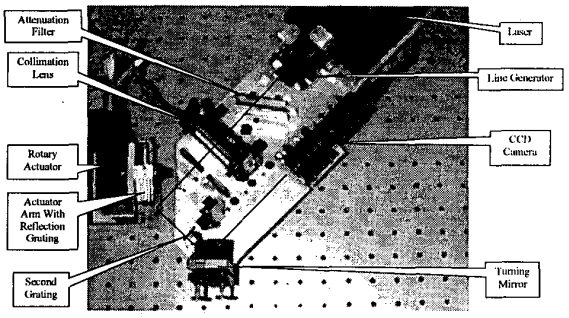

Figure 4. Top View of Breadboard Configuration

Figure 4 shows a top view of the rotary stage experimental setup, and the components described in §III can be seen. First, the linear light source is produced using a He-Ne laser, line generator optics, and cylindrical collimation lens. An attenuation filter may be necessary to prevent fringe pattern detector saturation. The linear laser source strikes the reflection grating with 20 μm period fixed to a HDD actuator arm mounted to the face of a rotary stage. The reflected diffracted beams pass through the second grating, which is a transmission grating with 16 μm period. The diffracted beams strike a turning mirror and are reflected to form the fringe pattern on the CCD camera.

Table 2. Statistics from Rotary Stage Stationary Test

	Unfiltered Data		Filtered Data	
	(nrad)	(encoder counts)	(nrad)	(encoder counts)
Angular displacement				
Actual	0	0	0	0
Calculated	316.9	1.6474	316.9	1.6474
Incr. Disp. Statistics				
Mean	0.0	0.00014	0.0	0.00014
Standard Deviation	347.4	1.80614	51.7	0.26885

To test the stability of the GI system, an experiment was done with the rotary stage stationary. Statistics found from data taken from this experiment appear in Table 2. For the unfiltered data, the calculated angular displacement was approximately 300 nrad, and the mean incremental displacement was negligible. To reduce the effects of noise, a low pass filter was applied to the quadrant values, which reduced the standard deviation of the incremental displacements.

A motion test was done with the rotary stage moving continuously through 4214 encoder counts to demonstrate

the motion tracking capability of the GI system. Figure 5(a) shows the quadrant values, which are periodic as expected for continuous motion. The recovered phase values in Figure 5(b) also follow a linear trend. A histogram of the incremental displacements appears in Figure 5(c) and most fall within ten encoder counts of zero.

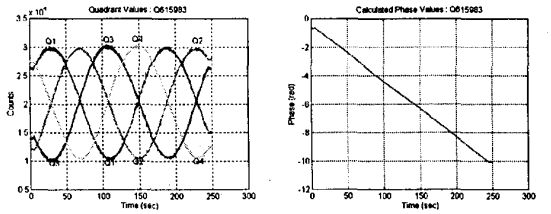

(a) Quadrant Values (b) Calculated Phase Values

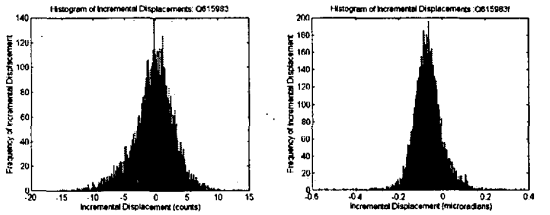

(c) Incr. Disp. Histogram (d) Filtered Incr. Disp. Histogram

Figure 5. Results for Rotary Stage Motion Test

Table 3. Statistics from Rotary Stage Motion Test

	Unfiltered Data	Filtered Data
Angular Displacement	**(encoder counts)**	**(encoder counts)**
Actual	4214	4214
Calculated	4346	~4214
Difference (% Diff)	132(3.13%)	~0(~0%)
Radius Value mm(in)	17.85(0.7027)	18.41(0.7247)
Incr. Disp. Statistics	**(encoder counts)**	**(encoder counts)**
Mean	-0.3596	-0.3487
Standard Deviation	3.1555	0.3566
Counts per Sample	0.3508	

Statistics calculated for unfiltered data from the motion test are in Table 3. Actual and calculated displacements vary by about three percent primarily due to the accuracy of the radius value of the light source, noise effects in the detector system, and stability of the light source intensity. The mean incremental displacement is quite small, but it has a significant standard deviation.

To reduce the effects of detector noise, the quadrant values for the motion test were filtered with a low pass filter. Figure 5(d) shows a histogram of filtered incremental displacements. Compared to the unfiltered histogram in Figure 5(c), the filtered values are skewed to the left of zero as expected for continuous motion. This indicates that the effects of detector noise have been significantly reduced to leave an accurate representation of the motion of the rotary stage as sensed by the detector. Statistics found for the filtered data are also in Table 3. For the filtered data an optimized radius value was used to reduce the error between the actual and calculated angular displacement values. Comparison of the incremental displacement statistics for the unfiltered and filtered data shows that the standard deviation for the filtered case is much less as expected. It is also significant that the mean incremental displacement value compares quite well with the counts per sample value indicating that the GI system was able to closely track motion of the rotary stage.

V. Conclusions and Future Work

An extension of the GI principle to the measurement of the angular displacement of a HDD actuator arm for use in the servo-track writing process has been presented. A number of experiments have been done with a prototype of the GI design to demonstrate the feasibility of the measurement system. Experimental results have shown that the system using a CCD camera as a fringe pattern detector is capable of generating stable signals and able to closely track the grating motion. Future enhancements that would be necessary for a production measurement system involve increasing both the measurement resolution and sampling rate. These objectives could be accomplished with either the use of smaller period grating combinations or a photodiode based fringe pattern detector.

VI. Acknowledgments

The research presented in this paper was supported in part by Maxtor Corporation through contract #E25-A09. The authors would also like to thank DVT, Inc. for providing the CCD camera system used in this research.

References

[1] B. Horwitz, "Diffractive techniques improve encoder performance," *Laser Focus World,* 143-8 (Oct. 1996)

[2] A. Teimel, "Technology and applications of grating interferometers in high-precision measurement," *Precision Eng.* **14**, 147-54 (1992).

[3] R. Freedland, "Laser interferometry positions disk drive heads," *Laser Focus World,* 108-9 (Dec. 1994)

[4] C. Lee, "Servowriters: A Critical Tool in Hard Disk Manufacturing," *Solid State Tech.*, 207-11 (May 1991)

[5] C. H. Bajorek and C. D. Mee, "Trends in storage technology through the year 2000," *Data Storage,* 23-30 (September 1994)

[6] B. Baker, "Non-Contact Servowriters," *Phase Metrics, Inc. Publication,* (September 1996)

[7] M. Bass, Handbook of optics, New York: McGraw-Hill; 1995. vol. 1 2.5-2.9.

[8] G. Voirin, O. Parriaux, H. Vuilliomenet, R. Wildi, U.Benner, and S. M. O. L. Schneider, "Using conventional photolithographic glass masks as high-efficiency phase gratings," *Optical Eng.* **34**(9), 2687-90 (September 1995)

[9] J-D Lin and H-B Kuo, "Development of a new optical scale system by the diffractive phase interference method," *Meas. Sci. Technol.* **6** 193-6 (1995)

[10] K. Creath, "Phase-measurement interferometry techniques," *Prog. Opt.* **26**, 349-93 (1988)